Coherence loss and recovery of an electron spin coupled inhomogeneously to a one-dimensional interacting spin bath: An adaptive time-dependent density-matrix renormalization group study

Zhi-Hui Wang,[1] Bing-Shen Wang,[2] and Zhao-Bin Su[1]
[1]*Institute of Theoretical Physics, Chinese Academy of Sciences, Beijing 100080, People's Republic of China*
[2]*State Key Laboratory of Semiconductor Superlattice and Microstructure and Institute of Semiconductor, Chinese Academy of Sciences, Beijing 100090, People's Republic of China*
(Received 13 February 2008; revised manuscript received 29 July 2008; published 21 August 2008)

Coherence evolution and echo effect of an electron spin, which is coupled *inhomogeneously* to an interacting one-dimensional finite spin bath via hyperfine-type interaction, are studied using the adaptive time-dependent density-matrix renormalization group method. It is found that the interplay of the coupling inhomogeneity and the transverse intrabath interactions results in two qualitatively different coherence evolutions, namely, a coherence-preserving evolution characterized by periodic oscillation and a complete decoherence evolution. Correspondingly, the echo effects induced by an electron-spin flip at time τ exhibit stable recoherence pulse sequence for the periodic evolution and a single peak at $\sqrt{2}\tau$ for the decoherence evolution, respectively. With the diagonal intrabath interaction included, the specific feature of the periodic regime is kept, while the $\sqrt{2}\tau$-type echo effect in the decoherence regime is significantly affected. To render the experimental verifications possible, the Hahn echo envelope as a function of τ is calculated, which eliminates the inhomogeneous broadening effect and serves for the identification of the different status of the dynamic coherence evolution, periodic versus decoherence.

DOI: 10.1103/PhysRevB.78.054433 PACS number(s): 75.40.Mg, 03.65.Yz, 03.67.Pp, 76.60.Lz

I. INTRODUCTION

Decoherence of a quantum object induced by an interacting spin bath rather than the conventional boson bath[1] is currently an attractive research subject. This interest stems mostly from the belief that electron spin is a promising candidate of qubit in scalable solid-state quantum computer architectures.[2,3] Recently the Hahn echo technique was also applied in measuring the decoherence of the localized electron spin. The rapid experimental progress in single spin measurements promises sensitive measurements of quantum dephasing effects in the near future.

For an electron spin embedded in a semiconductor matrix, in a proper range of external magnetic field and at low temperature, the dominant decoherence source is the temporally fluctuating random magnetic field originated from the dipolar interaction induced flip-flops of the surrounding nuclear-spin pairs. The electron spin dephasing due to this random magnetic filed then depends intimately on the quantum dynamics of the nuclear-spin bath. Such an intuitive dephasing mechanism can be properly described by the hyperfine (HF) interaction in association with the intrabath nuclear spin-spin interactions.

In Ref. 4, the authors reported a non-Markovian treatment for the dynamics of a localized electron spin coupled to a three-dimensional (3D) environment of nuclear spins solely via the HF interaction. Further works[5,6] stressed the importance of a quantum dynamic treatment for the intrabath spin interactions and developed a quantum cluster-expansion method (see also Ref. 7) to calculate the Hahn echo decay with its numerical results in good agreement with recent experiments.[8] Also, in Ref. 9, an intuitive pseudospin model was proposed for the pair interaction in the nuclear-spin bath and predicted a remarkable recoherence effect at time $\sqrt{2}\tau$ through disentanglement if the localized electron spin is flipped at time τ.

Almost in parallel, the decoherence of a central spin caused by a one-dimensional (1D) spin bath is becoming an alternative interesting subject. The 1D spin bath, e.g., an Ising or *XY* spin chain, has the advantage of being analytically solvable or allowing for more reliable simulations. It was suggested that the decoherence is subtly related to the characteristic status of the spin bath such as correlations, entanglement, and criticality.[10] For instance, a universal decoherence regime, which is independent of the system-bath coupling strength, was identified as a consequence of phase transition.[11]

In this paper we consider an electron spin coupled via HF-type interaction to an *interacting* 1D quantum spin chain, and employ the adaptive time-dependent density-matrix renormalization group (*t*-DMRG) technique to simulate the underlying quantum many-body dynamics. The model adopted in this work retains the basic ingredients of the quantum dephasing of an electron spin embedded in a mesoscopic 3D nuclear-spin bath, yet differs from the above mentioned 1D spin-bath models in that the electron spin is coupled *inhomogeneously* to all bath spins, where the inhomogeneity is crucial in the electron spin—bath spin coupling. We show that the interplay of the HF-type coupling inhomogeneity and the intrabath interactions lead to two kinds of qualitatively different behaviors for the electron-spin coherence evolution, namely, fully periodic and monotonically decaying evolutions, with a crossover regime in between. The former corresponds to a coherence-preserving phase, while the latter a complete decoherence phase.

Specifically, (i) the periodic free-induction evolution (FIE) carries a slow modulation with a superperiod commensurable to its basic period. The competition between the two

periods is responsible for the crossover to the decoherence evolution. In the decoherence evolution, the coherence decreases monotonically with an exponential decay index $k=4$. (ii) The echo effects induced by a sudden electron-spin flip show an additional recoherence peak sequence initiated at $t=\sqrt{2}\tau$ or $2\pi-\sqrt{2}(\pi-\tau)$ in the periodic regime and a single peak at $t=\sqrt{2}\tau$ in the decoherence regime. (iii) The periodic evolution is intrinsic and stable in sense that as the chain length increases, the basic period, the modulation superperiod, as well as the corresponding peak value maintain unchanged, while the peak width keeps shrinking with an interval of almost-zero coherence value emerging from the midpoint of each basic period. We suggest that the recoherence effect can be applied to explore the properties of periodic and decoherence evolutions with the same almost-zero coherence value. (iv) To render the experimental verifications possible, we show that the periodic versus decoherence evolution behaviors can be unshielded from the inhomogeneous broadening effect by the Hahn echo envelope at $t=2\tau$.

The rest of this paper is organized as follows: Sec. II is the physical background of our study. Section III is devoted to the motivations, 1D model, and calculation method. Section IV is the coherence evolutions in the single system dynamics (SSD). Here we denote SSD (Ref. 12) as the coherence evolution initiated from any state of the bath ensemble. Section IV A is for free-induction coherence evolution. Section IV B is for recoherence evolution. Section IV C is for the coherence loss (or coherence collapse) phenomena. In Sec. IV D, two variations of the primary model with modified HF-type interactions are studied. Section V is devoted to the ensemble average over the spin bath for the coherence evolution of the electron spin. Section VI is discussions and the concluding remarks. The appendix is devoted to the bath-size dependence of the periodic evolution.

II. PHYSICAL BACKGROUND

We consider the quantum dephasing, i.e., the coherence evolution, of an electron spin embedded in a nuclear spin-$\frac{1}{2}$ bath with a moderate to strong magnetic field applied. It can be described by the ensemble average of the off-diagonal matrix element of the electron spin $\hat{\mathbf{S}}_\alpha(\alpha=x,y)$, with the expression as

$$|\rho_{+-}(t)| = |\mathrm{Tr}[|-\rangle\langle+|\hat{U}^h(t)\hat{\rho}_0\hat{U}^{h\dagger}(t)]|. \tag{1}$$

This expression provides itself as a starting point to deal with both the free-induction coherence evolution and the spin-echo effect. Here, $\hat{\rho}_0=\hat{\rho}^e\otimes\hat{\rho}^N$ is the initial density matrix of the "electron spin-nuclear spin-bath" system. Moreover, $\hat{\rho}^e=|\Phi^S\rangle\langle\Phi^S|$ is the initial density matrix of the localized spin in a pure state $|\Phi^S\rangle$. $\hat{\rho}^N=\Sigma_n p_n|\Phi_n^0\rangle\langle\Phi_n^0|$ is that of the nuclear-spin bath where $\{|\Phi_n^0\rangle\}$ is a complete set of the nuclear-spin bath and $\{p_n\}$ is the corresponding probability distribution.

In Eq. (1), $\hat{U}^h(t)=\theta(\tau-t)\hat{U}(t)+\theta(t-\tau)\hat{U}(t-\tau)\hat{\sigma}_{x,e}\hat{U}(\tau)$ is the evolution operator with an instantaneous spin flip imposed to the electron spin at time τ and $\hat{U}(t)=e^{-i\hat{H}t}$ is the dynamical evolution operator of the "electron spin-spin bath" system. The total Hamiltonian

$$\hat{H} = |+\rangle\langle+|\left(\hat{H}_{Z_n}+\frac{1}{2}\Omega_e+\hat{H}_+\right)+|-\rangle\langle-|\left(\hat{H}_{Z_n}-\frac{1}{2}\Omega_e+\hat{H}_-\right), \tag{2}$$

with $|\pm\rangle$ being the eigenstates of the z component of the localized spin operator $\hat{\mathbf{S}}$, is decomposed into a direct sum of two parts, i.e., that projected to the electron spin-up subspace and that to the spin down. Moreover,

$$\hat{H}_\pm = \pm\hat{H}_0+\hat{V}_{dd}\pm\hat{V}_{\mathrm{hf}} \tag{3}$$

is the effective bath spin Hamiltonian conditioned on the electron-spin polarization.[5,6,9,12] In Eq. (3),

$$\hat{H}_0=\frac{1}{2}\sum_i A_i^{\mathrm{hf}}\hat{I}_i^z,$$

$$\hat{V}_{dd}=\sum_{i<j}\left[A_{ij}^{dd}\hat{I}_i^z\hat{I}_j^z+\frac{1}{2}B_{ij}^{dd}(\hat{I}_i^+\hat{I}_j^-+\hat{I}_i^-\hat{I}_j^+)\right],$$

$$\hat{V}_{\mathrm{hf}}=\frac{1}{2}\sum_{i<j}B_{ij}^{\mathrm{hf}}(\hat{I}_i^+\hat{I}_j^-+\hat{I}_i^-\hat{I}_j^+), \tag{4}$$

are the longitudinal hyperfine interaction, intrinsic dipolar nuclear-spin interaction, and the effective interaction mediated by the transverse hyperfine coupling with the electron, respectively. Ω_e is the Zeeman energy of the electron spin, while $\hat{H}_{Z_n}=\omega_I\Sigma_i\hat{I}_i^z$ the Zeeman energy of the nuclear spin with $\hat{I}_i^x=\frac{1}{2}(\hat{I}_i^+ +\hat{I}_i^-)$, $\hat{I}_i^y=\frac{1}{2i}(\hat{I}_i^+-\hat{I}_i^-)$ and $\hat{I}_i^z$ being the nuclear-spin operators on the ith site.

The coherence can be therefore expressed as

$$|\rho_{+,-}(t)| = \left|\langle\Phi^S|\hat{S}_x-i\hat{S}_y|\Phi^S\rangle\otimes\sum_n p_n\langle\psi_n^-(t)|\psi_n^+(t)\rangle\right|, \tag{5}$$

with

$$|\psi_n^\pm(t)\rangle = e^{-i\hat{H}_{Z_n}t}[\theta(\tau-t)e^{\mp i/2\Omega_e t}e^{-i\hat{H}_\pm t} + \theta(t-\tau)e^{\mp i/2\Omega_e(t-2\tau)}e^{-i\hat{H}_\pm(t-\tau)}e^{-i\hat{H}_\mp\tau}]|\Phi_n^0\rangle. \tag{6}$$

It shows that the non-Markovian quantum dephasing of an electron spin is due to the dynamical entanglement between the embedded spin and the bath (nuclear) spins such that the bifurcated pathways $|\psi_n^\pm(t)\rangle$ detach from each other far apart as $\langle\psi_n^-(t)|\psi_n^+(t)\rangle\to 0$. Yet, the coherence can also be restored by the disentanglement of the localized electron spin from the bath when the bifurcated pathways of the bath intersect at some later time, i.e., $|\psi_n^+(t)\rangle=|\psi_n^-(t)\rangle$.

In the solid-state quantum computer architectures, typical experiments would be carried out around the temperature $T\sim 100$ mK, which is low temperature for the electron but an extremely high temperature for the nuclear bath spin dynamics.[5,12] The ensemble average of the spin bath therefore should be taken into account to incorporate the extremely low excitation energy scale of the nuclear-spin bath.

Generally, the nuclear-spin excitation spectrum of a large system is the same up to a relative variance $\sim 1/\sqrt{N}$ (N being the total number of bath spins) for different initial states $|\Phi_n^0\rangle$.[12] Thus, the decoherence due to quantum fluctuations in

SSD $|\langle\psi_n^-(t)|\psi_n^+(t)\rangle|$ is insensitive to initial bath state when the system is sufficiently large and the temperature is appreciable for the nuclear spins. The coherence Eq. (5) can be therefore factorized into

$$|\rho_{+,-}(t)| = \mathcal{L}_{+,-}(t)\mathcal{E}_{av}(t), \tag{7}$$

where the Loschmidt echo $\mathcal{L}_{+,-}(t) \equiv |\langle\psi_n^-(t)|\psi_n^+(t)\rangle|$ reveals the dynamic entanglement between the electron and the nuclear spins in sense of SSD, and the ensemble average $\mathcal{E}_{av}(t) \equiv \Sigma_n p_n e^{-i\phi_n(t)}$ is the inhomogeneous broadening factor, with

$$\begin{aligned}\phi_n(t) &\equiv -\operatorname{Arg}[\langle\psi_n^-(t)|\psi_n^+(t)\rangle] \\ &= \theta(\tau - t)\left[\sum_j A_j^{\mathrm{hf}} I_{n,j}^z(t=0)\right]t \\ &\quad + \theta(t-\tau)\left[\sum_j A_j^{\mathrm{hf}} I_{n,j}^z(t=0)\right](t-2\tau).\end{aligned} \tag{8}$$

Obviously, as shown in Eq. (5), the Zeeman frequency of the electron spin Ω_e and nuclear spins $\hat{H}_{Zn}$ do not contribute to the coherence, so that the dynamics of the nuclear-spin bath described by the evolution operators $e^{-i\hat{H}_{\pm}t}$ maneuvers the coherence of the embedded electron spin.

III. 1D MODEL: MOTIVATIONS AND CALCULATION METHOD

To initiate our discussion, it is interesting to verify that the diagonal HF interaction contributed $\hat{H}_0$ can be put into the form as

$$\hat{H}_0 = \frac{1}{2N}\left(\sum_i A_i^{\mathrm{hf}}\right)\hat{I}^z + \frac{1}{2N}\sum_{i<j}(A_i^{\mathrm{hf}} - A_j^{\mathrm{hf}})(\hat{I}_i^z - \hat{I}_j^z). \tag{9}$$

Since $\hat{I}^z = \Sigma_i \hat{I}_i^z$ commutes with all terms in $\hat{H}_{\pm}$, Eq. (9) shows explicitly that $\hat{H}_0$ can be equivalently expressed as a sum of pairwise terms $(A_i^{\mathrm{hf}} - A_j^{\mathrm{hf}})(\hat{I}_i^z - \hat{I}_j^z)$ as far as Loschmidt echo is concerned. On the one hand, the physics of the longitudinal HF interaction in SSD depends only on the relative differences $\Delta A_{ij}^{\mathrm{hf}} = A_i^{\mathrm{hf}} - A_j^{\mathrm{hf}}$, i.e., it is not affected by the substitution $A_j^{\mathrm{hf}} \to A_j^{\mathrm{hf}} + \mathrm{cons.}$ for all sites. On the other hand, the dynamic evolution of the spin bath is then driven by four types of pairwise spin operators $\hat{I}_i^z - \hat{I}_j^z$, $I_i^+\hat{I}_j^-$, $\hat{I}_i^-\hat{I}_j^+$, and $\hat{I}_i^z\hat{I}_j^z$. In particular, for $I = \frac{1}{2}$, the former three form a SU(2) algebra satisfying

$$\begin{aligned}\left[\frac{1}{2}(\hat{I}_i^z - \hat{I}_j^z), \hat{I}_i^+\hat{I}_j^-\right] &= \hat{I}_i^+\hat{I}_j^-, \\ \left[\frac{1}{2}(\hat{I}_i^z - \hat{I}_j^z), \hat{I}_i^-\hat{I}_j^+\right] &= -\hat{I}_i^-\hat{I}_j^+, \\ [\hat{I}_i^+\hat{I}_j^-, \hat{I}_i^-\hat{I}_j^+] &= \hat{I}_i^z - \hat{I}_j^z,\end{aligned} \tag{10}$$

while $\hat{I}_i^z\hat{I}_j^z$ commutes with the other three terms in the spin-pair subspace.

Since the 1D model has the advantage of being analytically solvable or allowing for reliable precise simulations, to set up an 1D model from its 3D counterpart is often attractive and beneficial. It could be helpful to clarify some of the essential physics shared with the corresponding 3D physical system. It might also enrich the understanding of the quantum dynamics of the decoherence of a central spin caused by 1D spin bath itself. The observations in the above paragraph form a guideline in extracting a 1D model from the decoherence of an electron spin embedded in a 3D mesoscopic nuclear-spin bath.

For a 3D quantum dot, A_j^{hf} is proportional to the modulus square of the electron wave function at site j in which the difference $\Delta A_{ij}^{\mathrm{hf}}$ varies significantly site to site. As the longitudinal HF coupling plays a major role in the electron-spin-bath interaction, to keep its distinctive feature of spatial inhomogeneity in our 1D model, we would like to take $\Delta A_{ij}^{\mathrm{hf}} = \Delta A^{\mathrm{hf}}(j-i)$ with ΔA^{hf} being constant as a minimal model, i.e.,

$$A_j^{\mathrm{hf}} = (N-j)\Delta A^{\mathrm{hf}} + A_N^{\mathrm{hf}}. \tag{11}$$

Moreover, the transverse HF interaction contributed effective intrabath interaction is external magnetic-field dependent. For a typical semiconductor quantum dot with field strength $10-1T$,[6,12] it has an energy scale of $B_{ij}^{\mathrm{hf}} \sim 1-10\ \mathrm{s}^{-1}$. Meanwhile that of the near-neighbor dipolar intrabath interaction is $B_{ij}^{dd} \sim 10^2\ \mathrm{s}^{-1}$. The former is much smaller than that of the longitudinal part by an order of $A_i^{\mathrm{hf}}/\Omega_e$; it is also smaller than the latter by an order of 10. We therefore neglect the extrinsic nuclear-spin interaction and set $B_{ij}^{\mathrm{hf}} = 0$. We further take the intrinsic dipolar interaction to be nearest-neighbored as $B_{ij}^{dd} = B^{dd}\delta_{i,j\pm1}$ and $A_{ij}^{dd} = A^{dd}\delta_{i,j\pm1}$. Then the electron spin conditioned effective bath Hamiltonian becomes

$$\begin{aligned}\hat{H}_{\pm} = \frac{\Delta A^{\mathrm{hf}}}{2}\Bigg(&\mp\sum_{j=1}^{N} j\hat{I}_j^z + \frac{1}{\xi}\Bigg[\sum_{j=1}^{N-1} -(\hat{I}_j^+\hat{I}_{j+1}^- + \hat{I}_j^-\hat{I}_{j+1}^+) \\ &+ 2\eta\hat{I}_j^z\hat{I}_{j+1}^z\Bigg]\Bigg) \pm \left(\frac{A_N^{\mathrm{hf}} + N\Delta A^{\mathrm{hf}}}{2}\right)\hat{I}^z.\end{aligned} \tag{12}$$

Now the dynamic evolution of the quantum coherence can be characterized by dimensionless parameters $\xi \equiv \Delta A^{\mathrm{hf}}/(-B^{dd})$ and $\eta \equiv A^{dd}/(-B^{dd})$, with the time variable t normalized by $4/\Delta A^{\mathrm{hf}}$ (throughout the paper). In sum, such extracted 1D system retains the essential features of its 3D counterpart, e.g., the monotonically descending spatial inhomogeneity of the longitudinal HF interaction, the pairwise SU(2) algebra, and that the sign of $\hat{H}_0$ is conditioned on the embedded electron-spin state. The t-DMRG method[13] is available and can be properly applied to simulate the time evolution with enough precision.

In our t-DMRG calculations, the chain length is taken as $N = 50$, 100, 150, 200, and 250, with properly chosen hundreds of truncation states being kept. Since, as shown in the Appendix, the coherence evolution is stabilized after $N \gtrsim 30$, the calculations in our manuscript are proceeded with $N = 50$ if not specified. The Trotter-Suzuki decomposition[14] is held up to the second order. If $\xi = 100$, the time step is chosen

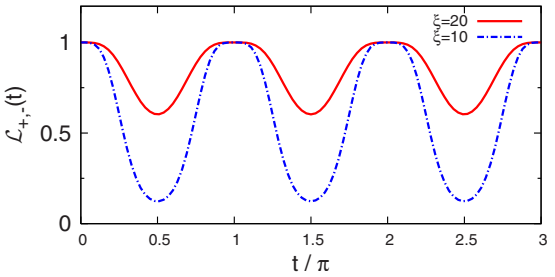

FIG. 1. (Color online) Free-induction coherence evolution in the periodic regime with $\xi=10,20$ and $A^{dd}=0$. The time is normalized by $4/\Delta A^{\mathrm{hf}}$. The evolution exhibits a basic periodic π.

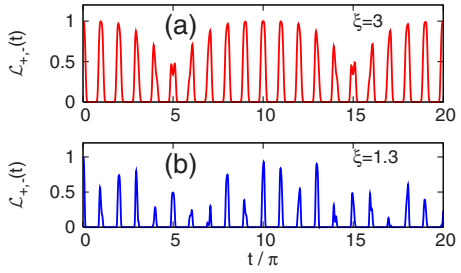

FIG. 2. (Color online) Crossover behavior of free-induction coherence evolution with $A^{dd}=0$. (a) For $\xi=3$, the periodic evolution carries a modulation with period $10T_{dd}$. (b) For $\xi=1.3$, the peaks at $t=mT_{dd}$, $m=1,2,\ldots$ oscillate irregularly.

as $\Delta t\sim 10^{-2}$; the numerical precision can be maintained for 10^4 time steps. Our initial bath states are prepared as the eigenstates of the Zeeman energy of the bath by an independent DMRG calculation,[15] where off-diagonal coherence is absent.

IV. SINGLE-SYSTEM DYNAMICS

A. Free-induction coherence evolution in single-system dynamics

We initiate our discussion from the single state coherence evolution in which the initial bath spin state is taken as any of the eigenstates of the Zeeman energy of the bath spin.

For simplicity, we first take the longitudinal intrabath interaction as $A^{dd}=0$. We find that the coherence evolution is controlled by two kinds of distinct behaviors: the periodic evolution in the regime with ξ large enough and the decoherence evolution with ξ small enough. The gradient of the longitudinal HF interaction ΔA^{hf} favors the periodic evolution while the intrabath spin interaction causes decoherence.

For $\xi\gg 1$, see $\xi=10$ in Fig. 1, the coherence evolution exhibits a periodic oscillation versus the reduced time with a generic period $T_{dd}\cong\pi$ independent of ξ. It shows also a mirror symmetry with respect to the midpoint of each period.

Moreover, if we attend to the time scale of the order of $\xi(\gg T_{dd})$, we find that the oscillating evolution carries a slow modulation with a superperiod T_{sup} locked at an integer multiplier of T_{dd} as

$$T_{\mathrm{sup}}\cong(1+[\xi^2]^{\mathrm{fl,ce}})T_{dd}, \tag{13}$$

where the superscript "fl" means the floor function and "ce" the ceiling function. For any real number x, we denote the integer closest to x by $[x]^{\mathrm{fl,ce}}$. The coexistence of two mutually commensurate periodicities is essentially the consequence of two kinds of energy scales as that of the HF interaction and that of the intrabath interaction. When ξ is large enough ($\Delta A^{\mathrm{hf}}\gg B^{dd}$), such slow modulation does not affect the above discussions which mainly extend only a few T_{dd} periods. When ξ gets down to the lower brim of the periodic regime, as a precursor of the crossover zone, the modulation becomes palpable and is then responsible for the evolution periodicity, see Fig. 2(a).

With the further decrease of ξ, the superperiod becomes comparable to T_{dd} and its periodicity starts to disappear, i.e., its peak sequence starts to decay in a chaotic way, see Fig. 2(b). The time scale of the basic period T_{dd} appears quite robust such that its remnant persists even up to the peripheric regime of the decoherence evolution.

When ξ is small enough, the coherence attenuates monotonically approaching zero within a time interval t_d and will not rise up perceptibly any more, see Fig. 3(a). The decoherence time evolution can be fitted as an exponential function of minus t to the power k with $k=4$, see Fig. 3(b). Such decoherence behaviors in our 1D model are in excellent consistence with those deducted from the pseudospin model in 3D.[12]

Now we further introduce the diagonal spin-spin interaction with $A^{dd}=-2B^{dd}$ ($\eta=2$), which is consistent with the nuclear intrinsic dipole-dipole interaction.[6] The coherence evolution still exhibits two types of qualitatively different behaviors, i.e., periodic oscillation and complete decoherence evolution.

In the periodic regime, although the diagonal interaction constant A^{dd} is of the same order of magnitude with that of B^{dd}, it makes the modulation considerably strengthened with the modulation period shortened and its amplitude enhanced. Instead of $([\xi^2]^{\mathrm{fl,ce}}+1)T_{dd}$ as in the case of $A^{dd}=0$, the modulation period becomes much smaller as

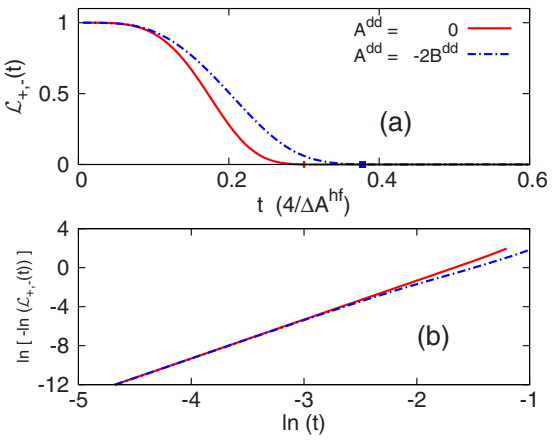

FIG. 3. (Color online) (a) Free-induction coherence evolution in the decoherence regime for $\xi=0.5$, with $A^{dd}=0$ (red solid line) and $A^{dd}=-2B^{dd}$ (blue dashed line). The coherence decreases monotonically. Coherence disappearing time t_d is labeled on the t axis. (b) Logarithmic plot for (a). The exponential decay indices are $k=4$ for both evolutions.

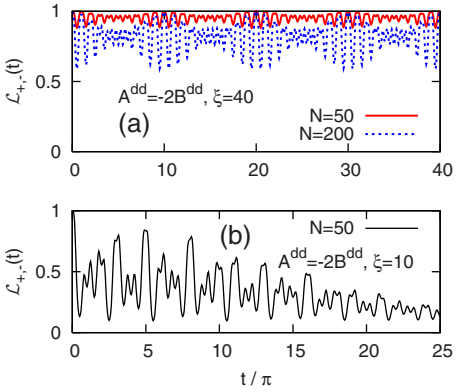

FIG. 4. (Color online) Free-induction coherence evolution with $A^{dd}=-2B^{dd}$. (a) Modulation in the periodic regime with $\xi=40$ for $N=50,200$. For $A^{dd}=0$ (not shown here), the modulation on the periodic evolution is negligible [see Eq. (13)] while here, with A^{dd} included, the modulation is strengthened to $T_{\rm sup}\cong 20T_{dd}$. The superperiod $T_{\rm sup}$ is not affected by chain length. (b) For $N=50$, $\xi=10$, the evolution enters the crossover regime already.

$$T_{\rm sup}=\left[\frac{\xi}{2}\right]^{\rm fl,ce}T_{dd}, \tag{14}$$

see Fig. 4(a).

The inclusion of the diagonal intrabath interaction encroaches the periodic regime of the case with $A^{dd}=0$ and extends the crossover regime. Take $\xi=10$ as an example, instead of exhibiting typical periodic behavior with $A^{dd}=0$, the peak sequence of the coherence evolution decays in a chaotic way with $A^{dd}=-2B^{dd}$ included, see Fig. 4(b).

In the decoherence regime, the coherence evolution behavior is very close to that with $A^{dd}=0$; it keeps not only almost same coherence disappearing time t_d, but also the same decay index $k=4$, see Fig. 3.

B. Recoherence effects in single-system dynamics

We then impose a sudden electron-spin flip to the coherence evolution at $t=\tau$ and consider the case $A^{dd}=0$ first. For the periodic evolution, with $\tau\in(0,T_{dd}/2)$, it would yield an additional periodic pulse sequence at $\sqrt{2}\tau+nT_{dd}$ with $n=0,1,\ldots$. Meanwhile, those coherence peaks in the absence of spin flip still survive but, due to the intervention of the spin flip, experience a phase delay $\Delta\phi(\tau)$ and shift to $t=\Delta\phi(\tau)+mT_{dd}$ with $m=1,2,\ldots$, see Fig. 5. For $\tau\in(T_{dd}/2,T_{dd})$, the recoherence evolution is found to be the reflection image of that resulting from spin flip at $T_{dd}-\tau$, so that the recoherence peak sequence initiates at $2T_{dd}-\sqrt{2}(T_{dd}-\tau)$ and $\Delta\phi(\tau)=-\Delta\phi(T_{dd}-\tau)$, see Fig. 5(a). This behavior is a direct consequence of the mirror symmetry of the free-induction periodic evolution, with respect to reflection points $(n+1/2)T_{dd}$. We further realize that, as expected, the recoherence evolution exhibits the same superperiod as that of the free-induction evolution.

In the decoherence regime, the recoherence signal closely depends on the time τ when the spin flip is imposed. As long as $\tau<t_d$, the recoherence pulse will peak at $t=\sqrt{2}\tau$ with the coherence fully recovered as shown in Fig. 6(a). However, if

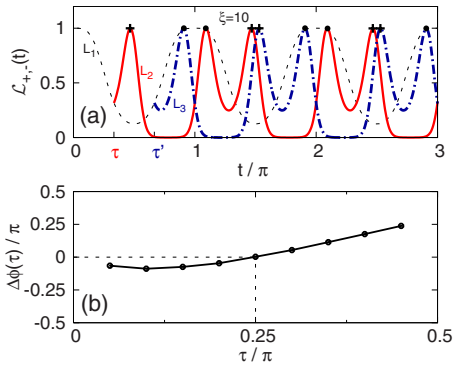

FIG. 5. (Color online) Recoherence behavior in the periodic regime with $\xi=10$. (a) Coherence evolutions without spin flip (L_1) and with spin flip at $\tau=T_{dd}/3$ (L_2), and $\tau'=T_{dd}-\tau$ (L_3). The recoherence peaks and intervened original peaks are labeled on the lines as crosses and filled circles, respectively. After $t>\tau'$, L_2 and L_3 show a mirror symmetry with respect to reflection points $t=n\pi/2$ with $n=2,3,\ldots$. (b) The phase shift $\Delta\phi$ as a function of τ with $\tau\in(0,T_{dd}/2)$. $\Delta\phi(\tau)$ changes sign at $t=T_{dd}/4$ at which $\Delta\phi=0$.

the spin flip time τ exceeds t_d, the coherence recovers still at $\sqrt{2}\tau$ but damps quickly, see solid lines in Fig. 6(b).

With the longitudinal spin-spin interaction included $A^{dd}=-2B^{dd}$, in the periodic regime, the recoherence behavior exhibits similar evolution to that with $A^{dd}=0$. The recoherence peak sequence experiences the same enhanced modulation as in the case without spin flip. In the decoherence regime, however, even with the spin flip exerted within t_d, with increase τ, the peak value at $\sqrt{2}\tau$ decreases considerably faster than that without A^{dd}, as shown in Fig. 6 by the dashed lines.

To our understanding, the above calculated $\sqrt{2}\tau$-type spin-echo effect validates the intuitive mechanism of the recoherence effect proposed in Ref. 12 for a mesoscopic 3D quantum dot. Yet the diagonal intrabath interactions considerably weaken the recoherence effect in the decoherence evolution in 1D case.

C. Coherence loss versus coherence preserving

We have studied the bath-size dependence of the coherence evolution in detail starting from $N=2$, see the Appen-

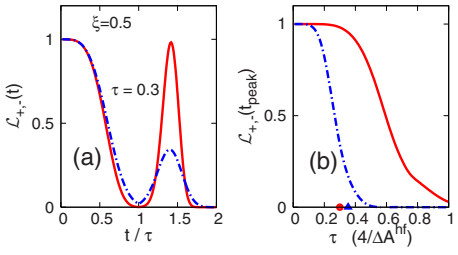

FIG. 6. (Color online) Recoherence evolution in the decoherence regime for $\xi=0.5$, $A^{dd}=0$, (solid lines), and $A^{dd}=-2B^{dd}$ (dashed lines). (a) The coherence peaks at $\sqrt{2}\tau$. (b) The peak value $\mathcal{L}_{+,-}(t_{\rm peak})$ as a functions of τ. The coherence disappearing times t_d's are labeled on the τ axis in the same color with the corresponding curves.

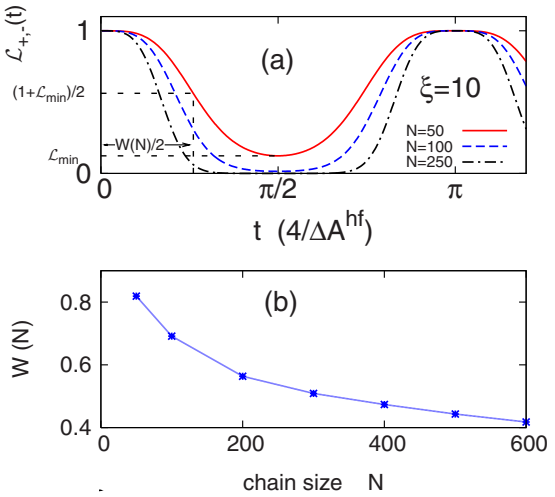

FIG. 7. (Color online) Effect of chain size N on the basic periodicity in the periodic regime $\mathcal{L}_{+,-}(t)$. (a) For $\xi=10$, $A^{dd}=0$, when N varies from 50 to 250, the oscillating period T_{dd} is independent of chain size. $W(N)$ labels the width of the coherence peak. (b) The width of the peak $W(N)$ defined in (a) as a function of the bath chain size.

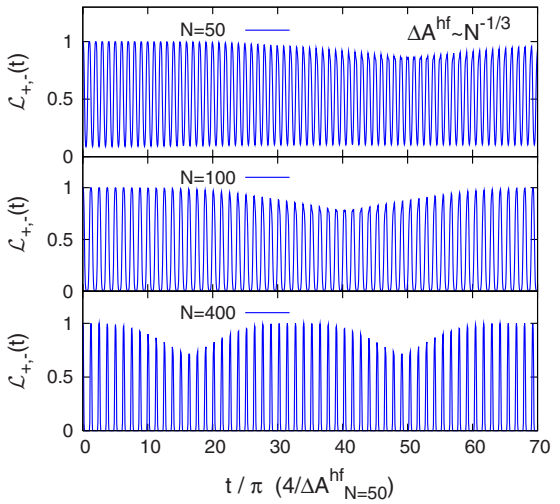

FIG. 9. (Color online) Coherence evolution in the periodic regime with $\Delta A^{\mathrm{hf}} \propto N^{-1/3}$, with chain sizes $N=50$, 100, and 400. Time unit is taken as ΔA^{hf} when $N=50$. The effective ξ equals 10, 8, and 5, respectively. Accordingly, the superperiod shrinks as the chain size increases.

dix. We realize that, when the chain size N exceeds 30 sites, the coherence evolution in the periodic regime becomes stable in sense that, the basic period, the modulation superperiod, as well as the corresponding peak value maintain unchanged. Meanwhile, the dip of each basic period moves down gradually and the width of the peak keeps shrinking as the chain length increases, see Fig. 7.

Such shrinking of the peak width of the periodic coherence evolution is essentially a distinctive feature sharing with the Hepp-Coleman type models.[16–21] In particular, after the coherence at the dip of each period drops down to a value close to zero, an interval with almost-zero coherence value emerges from the dip and stretches to both sides within each period. In fact, in the Hepp-Coleman type models, the evolution operator can be factorized into a continued multiplication over chain sites due to the noninteracting character of the spin bath. What we have here is an interacting spin bath with its evolution operator cannot be factorized.

Such almost-zero coherence resulted from the successive separation of the bifurcated pathways was often regarded as an indication of the loss of coherence.[17,22] However, if a spin flip is imposed to the electron at time τ within the almost-zero coherence interval for the periodic evolution, the spin flip will always induce a peak sequence with its coherence value fully recovered, see Fig. 8. Yet, in the decoherence regime, if the spin flip is exerted at a time when the coherence value is as small as those in the zero-coherence interval, no prominent recoherence signal can be induced.

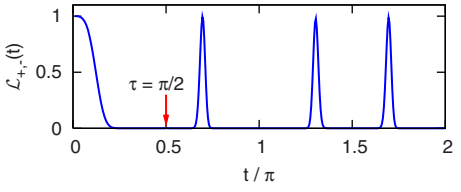

FIG. 8. (Color online) Recoherence evolution for $N=200$, $\xi=5$. The spin flip is exerted when the coherence value is almost zero.

We therefore have the understanding that the periodic evolution is coherence preserving in sense that the spin-flip operation always induces a stable recoherence peak sequence, while the decoherence evolution with the coherence monotonically decreasing is actually a coherence-losing process. Our model accommodates these two qualitatively different coherence evolutions connected by a continuous crossover and under the control of the competition between the electron spins—bath interaction and the intrabath interaction.

D. Extension of the minimal model

Besides the study in the above subsections, it is also interesting to examine the effect of relaxing the condition of constant $\Delta A^{\mathrm{hf}}_{j,j+1}$, i.e., Eq. (11) in our minimal model.

We first consider the case with ΔA^{hf} being chain-size dependent $\Delta A^{\mathrm{hf}} \propto N^{-1/3}$ but maintaining itself as a site-independent constant. In Appendix, we have numerically verified that the coherence evolution is stable with the increase of bath chain. In the present case, as chain size increases, the slope of the hyperfine interaction decreases. We calculated the coherence evolution for $N=50$, 100, and 400, with $\Delta A^{\mathrm{hf}}=(50/N)^{1/3}$ and fixed $B^{dd}=-0.1$. The results are shown in Fig. 9. For $N=50$, the evolution parameter is $\xi=10$; the coherence evolution exhibits typical periodic behavior. As bath size increases, the superperiod of the periodic evolution shrinks since the effective ξ decreases as chain length extends. Therefore, it can be understood that as the chain size increases, due to the decreasing of the inhomogeneity of the HF interaction, the system shows up a tendency from periodic oscillation to crossover into a decoherence evolution.

We now consider the effect of the site dependence of $A^{\mathrm{hf}}_{j,j+1}$. Along certain crystalline symmetry axis,[23] the wave

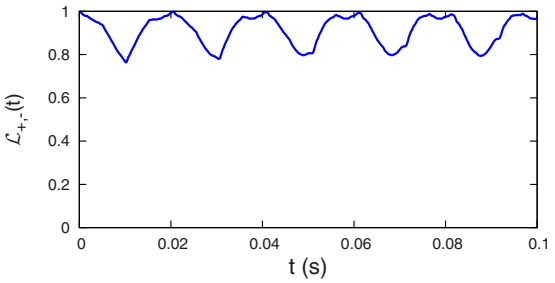

FIG. 10. (Color online) Coherence evolution with $A_j^{\rm hf}=\tilde{A}^{\rm hf}\cos^2\frac{(j-1)\pi}{2N}$ in the coherence-preserving regime with $B^{dd}=100\ \mathrm{s}^{-1}$ and $A^{dd}=0$. For $N=200$, $\tilde{A}^{\rm hf}=2\times10^7\ \mathrm{s}^{-1}$, the coherence oscillates with its value close to unity.

function of the embedded electron in a 3D quantum dot has the form of a cosine function. We take $A_j^{\rm hf}=\tilde{A}^{\rm hf}\cos^2\frac{(j-1)\pi}{2N}$. Then, $\Delta A_{j,j+1}^{\rm hf}$ varies from site to site on the lattice chain and the average slope of $A_j^{\rm hf}$ is chain-size dependent for a given $\tilde{A}^{\rm hf}$. Take the chain length $N=200$ and $B^{dd}=10^2\ \mathrm{s}^{-1}$. If $\tilde{A}^{\rm hf}$ is set as $2\times10^7\ \mathrm{s}^{-1}$, we find that the periodicity disappears due to the lack of a unified time normalization $\Delta A^{\rm hf}$, although the site-dependent $\Delta A_{j,j+1}^{\rm hf}/B^{dd}$ is of the order 200, which falls into the periodic regime of our primary model. Nevertheless, interestingly, the nonperiodic coherence evolution keeps oscillating close to unity without decaying, see Fig. 10. For $\tilde{A}^{\rm hf}=10^5\ \mathrm{s}^{-1}$, $\Delta A_{j,j+1}^{\rm hf}/B^{dd}$ is of the order 1, the coherence and recoherence evolutions behave almost the same way as their counterparts in decoherence regime of our primary model, see Fig. 11. We stress that the larger the chain size N, the larger $\tilde{A}^{\rm hf}$ is required to stay in the coherence-preserving regime. For any chain size N (at least within our calculation experience), the nondecaying coherence-preserving regime always exists if we choose $\tilde{A}^{\rm hf}$ large enough.

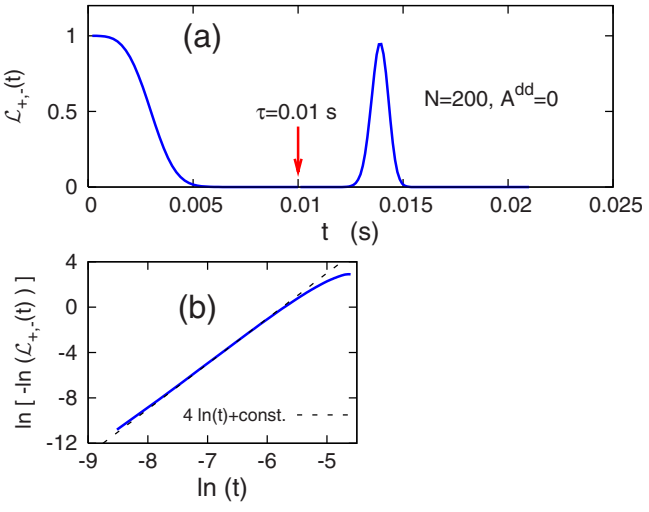

FIG. 11. (Color online) For $N=200$ with $A_j^{\rm hf}=\tilde{A}^{\rm hf}\cos^2\frac{(j-1)\pi}{2N}$, $\tilde{A}^{hf}=10^5\ \mathrm{s}^{-1}$, $B^{dd}=100\ \mathrm{s}^{-1}$, and $A^{dd}=0$. (a) Recoherence evolutions behave similar to that in the decoherence regime of our primary model. (b) Logarithmic plot of coherence evolution in (a) before spin flip; the evolution also exhibits quartic exponential coherence decay.

In fact, in a 3D quantum dot, the wave function of the embedded electron extends over the whole dot with a normalization factor inversely proportional to the square root of the dot volume. The longitudinal HF interaction $A_j^{\rm hf}$, which is proportional to the modulus square of the electron wave function at site j,[24] is then not only dependent on the specific form of the wave function site by site, but also dot-volume dependent. The above two variations on the HF-type interaction in our 1D model resemble these two aspects of the 3D quantum dot.

The discussions in this section imply that, for a general class of inhomogeneous interaction, the dynamic coherence evolution is still under the control of two fix points, i.e., a decoherence regime with its whole feature kept as in our primary model, and corresponding to the periodic regime, a quantum chaotic regime instead, in which the coherence sustains a nondecaying irregular oscillation.

V. INHOMOGENEOUS BROADENING AND HAHN ECHO ENVELOP

The single system dynamics studied in Sec. IV exhibits various important features of the quantum dynamic entanglement process. Yet, these interesting properties could be shielded by the inhomogeneous broadening effect contributed by the ensemble average $\mathcal{E}_{av}(t)$. It is then desirable to limit the bath spin configurations experimentally to observe the SSD.

Nonetheless, if an electron-spin flip is imposed at time τ, the broadening effect due to phase accumulation will be canceled as $\mathcal{E}_{av}(2\tau)=1$ at $t=2\tau$, see Eq. (8). The coherence $|\rho_{+,-}(2\tau)|$ then results solely from the dynamic quantum entanglement as

$$|\rho_{+,-}(2\tau)|=\mathcal{L}_{+,-}(2\tau) \tag{15}$$

and serves an exposure of the quantum coherence evolution in SSD. We plot $|\rho_{+,-}(2\tau)|$ as functions of τ in Fig. 12. In the periodic regime, the recoherence evolutions induced by spin flip exerted at τ and $\tau+T_{dd}$, respectively, are shown for comparison. Since the coherence status at τ and $\tau+T_{dd}$ are the same, and the recoherence evolutions are also periodic with period T_{dd}, we realize that the Hahn echo signal as a function of 2τ is periodic with a period $2T_{dd}$. We further provide two examples to illustrate its physical implications, see dashed lines in Fig. 12. In the decoherence regime, the Hahn echo exhibits a quartic exponential decay as shown in Fig. 12(b), consistent with that reported in 3D case.[12] Therefore, in virtue of the Hahn echo technique, we can detect the two qualitatively different dynamic coherence evolutions in SSD.

We notice that, if $A_N^{\rm hf}$ can be adjusted to be $A_N^{\rm hf}=m\Delta A^{\rm hf}$, $m=0,1,\ldots$, the inhomogeneous broadening factor $\mathcal{E}_{av}(t)$ will be refocused to 1 at $t=mT_{dd}/2$, which would provide directly exposures of coherence evolution in SSD without spin flips.

VI. CONCLUDING REMARKS

In this paper, we studied the coherence evolution of an electron spin interacting with a 1D finite spin chain via inhomogeneous hyperfine-type coupling. This model is ex-

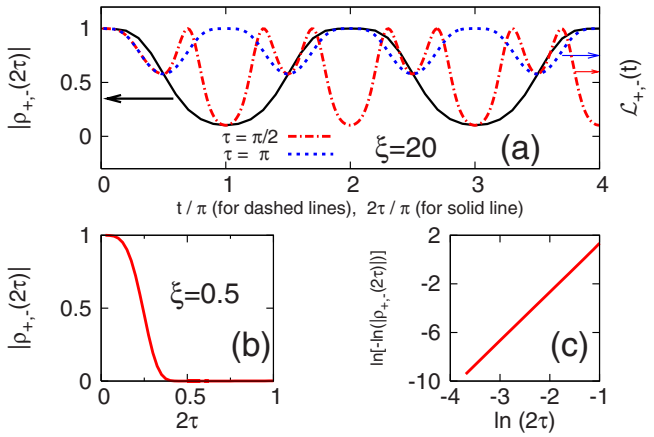

FIG. 12. (Color online) Hahn echo envelope $|\rho_{+,-}(2\tau)|$ as functions of 2τ with $A^{dd}=0$. High-temperature approximation for the nuclear-spin bath ensemble is taken as $p_n=$const. (Refs. 5 and 12). (a) For $\xi=20$, $|\rho_{+,-}(2\tau)|$ (solid line) is a periodic function with period $2T_{dd}$. The short-dashed line is the recoherence evolution in SSD for $\tau=T_{dd}$, where the spin-flip effects virtually disappears; it intersects the Hahn echo envelope at $t=2nT_{dd}$, $n=1,2,\ldots$. The long-dashed line is for $\tau=T_{dd}/2$ and intersects the Hahn echo envelope at nT_{dd}. (b) and (c) show that for $\xi=0.5$, the Hahn echo signal exhibits a quartic exponential decay.

tracted from its 3D counterpart: an electron spin dephases due to the interaction with the nuclear spins in a mesoscopic 3D quantum dot.

We realized that in our model, the dynamic evolution of the electron-spin coherence manifests a continuous crossover from a periodic to a decoherence evolution within our numerical precision. The periodic evolution carries a modulation with a commensurate superperiod, and the competition between the two periods is responsible for the crossover. The counterpart of the periodic evolution in our model was not found in the 3D case. The decoherence evolution as well as its $\sqrt{2}\tau$-type echo effect validates most of the distinctive features resulted from the pseudospin model or cluster-expansion method for a 3D quantum dot.

We included the longitudinal intrabath spin-spin interaction. Physically, it is a kind of scattering term between the collective excitations and provides a decoherence-favorable mechanism. We found that the system still exhibits periodic evolution as long as the deep inhomogeneity of HF-type interaction dominates. In the decoherence regime, the longitudinal interaction has little effect on the free-induction evolution, but would significantly affect the $\sqrt{2}\tau$-type echo effect.

As the bath size increases, the periodic evolution shows up a "loss of coherence" phenomena, i.e., an interval with almost-zero coherence value emerges from the midpoint and stretches to both sides within each evolution period. Nevertheless, by imposing the spin-echo effect, we learn that the periodic evolution is essentially a coherence-preserving evolvement while the decoherence evolution is a coherence-losing process.

We investigated two variations of our primary model with modified hyperfine-type interaction. The dynamic coherence evolution still exhibits two kinds of qualitatively different behaviors.

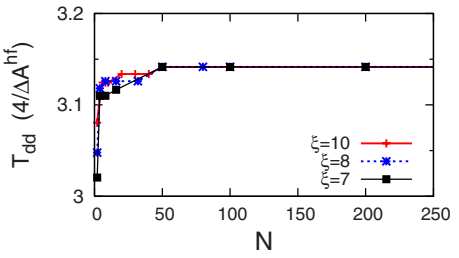

FIG. 13. (Color online) Basic period T_{dd} as a function of chain size N for 8 and 7 with $A^{dd}=0$. The initial configuration of the bath spin is randomly picked.

In case the proposed 1D system can be realized experimentally, e.g., by applying the optical lattice manipulation techniques to cold atom system,[25] the Hahn echo type refocusing effect could then unveil the rich phenomena in single-system dynamics.

As final remarks, we would like to stress that an increase in the gradient of hyperfine interaction $\Delta A^{hf}_{j,j+1}$ is in favor of keeping the coherence evolution in the periodic regime. Therefore, steepening the inhomogeneity of the wave function of the embedded electron could be favorable to preserve the coherence. This might shed light on the materialization of prolonging the quantum coherence time of the embedded electron spin. Moreover, for the evolution status with the same almost-zero coherence values, the different responses to the electron-spin flip suggest an unexplored and rather intriguing aspect of the coherence description for the electron spin interacting with a nuclear-spin bath.

ACKNOWLEDGMENTS

We are grateful to Chang-Pu Sun for bringing our attentions to this interesting topic and to Xin-Qi Li and Hui Tang for helpful discussions.

APPENDIX: CHAIN-LENGTH DEPENDENCE OF THE PERIODIC EVOLUTION

It is crucial to verify that in the regime of $\xi \gg 1$, the periodic coherence evolution is stable with the increase of the chain length.

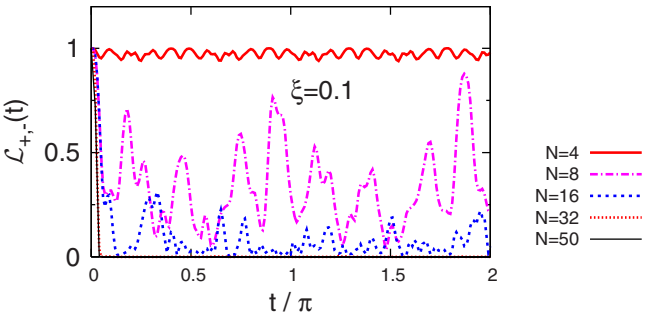

FIG. 14. (Color online) Coherence evolution for different bath size with $\xi=0.1$ and $A^{dd}=0$. The decoherence evolution comes into being for $N>30$.

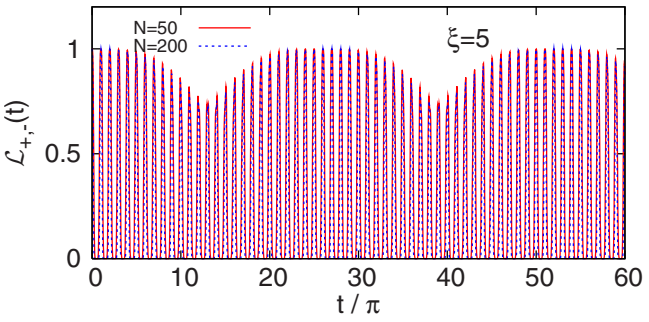

FIG. 15. (Color online) Modulation on the periodic evolution for $N=50$, 250 with $\xi=5$ and $A^{dd}=0$. The superperiod is not affected by chain length.

We first consider the chain-length dependence of the periodic evolution for N being small. For convenience, we take $A^{dd}=0$ and focus on the first few periods. We have exact solution for the electron spin interacting with a 2-sites nuclear-spin bath, the solved basic period is $T_{dd}(N=2)=\pi/\sqrt{1+4/\xi^2}$. As the chain size increases from $N=2$, our numerical calculations show that, see Fig. 13, the basic period increases correspondingly and stabilizes at a value π for $N\gtrsim 30$ approximately, which is independent of ξ. Moreover, the superperiod is also stable for $N>2$. For comparison, we consider additionally the coherence evolution beyond the periodic regime with, e.g., $\xi=0.1$. As shown in Fig. 14, for $N\gtrsim 30$, the decoherence evolution appears as a monotonically decaying evolution with an exponential decay index $k=4$. The corresponding calculation proceeds over 100π without any coherence revival effect. These two mutually complemented aspects indicate that the coherence evolution is indeed stable for chain length $N\gtrsim 30$. The calculated various properties of the coherence evolution for $N\geq 50$ are intrinsic.

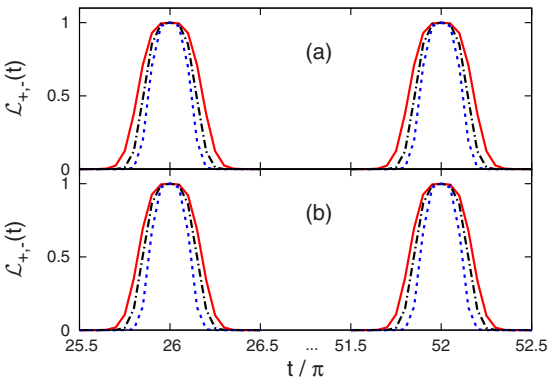

FIG. 16. (Color online) Modulation on the periodic evolution with $A^{dd}=0$ for $\xi=5$. The first two peaks of the supermodulation at $t=T_{\rm sup}$ and $t=2T_{\rm sup}$ are shown in detail. The results for two randomly selected initial-state configurations are shown in (a) and (b). In each subfigure, curves from outside to inside are for $N=50$, 100, and 250, respectively. The superperiod is not affected by chain length; the peak value of the supermodulation is kept at unity.

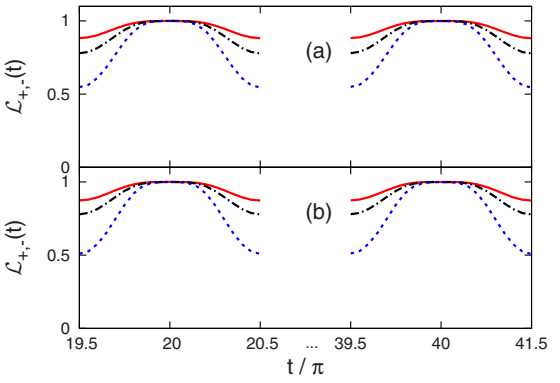

FIG. 17. (Color online) Modulation on the periodic evolution with $A^{dd}=-2B^{dd}$ for $\xi=40$. The first two peaks of the supermodulation at $t=T_{\rm sup}$ and $t=2T_{\rm sup}$ are shown in detail. The results for two randomly selected initial-state configurations are shown in (a) and (b). In each subfigure, curves from outside to inside are for $N=50$, 100, and 250, respectively. The superperiod is not affected by chain length. The peak value of the supermodulation is kept at unity.

We further investigate the bath-size dependence of periodic evolutions with $N=50,100,\ldots,250$. We choose relatively large ξ to filter the effect of the supermodulation and find that not only the basic period π but also the peak value of the oscillating coherence is kept unchanged, see Fig. 7, i.e., the T_{dd} periodicity is robust against the extending of chain length. On the other hand, the dip of each oscillation period moves down gradually, and the width of the peak keeps shrinking as the chain length increases, see Fig. 7.

We further attend to the long-time behavior of the periodic evolution. As shown in Fig. 15, the supermodulation periodicity still keeps unchanged with the increase of chain length, and the peak value of the coherence evolution, which occurs at the nodes of the supermodulation, maintains at unity, see Fig. 16.

We now take the diagonal interaction $A^{dd}=-2B^{dd}$ into consideration. As the chain size increases, although the amplitude of the modulation increases as shown in Fig. 4, the superperiod keeps invariant, and the peak value of the supermodulated coherence evolution maintains unchanged as in the case with $A^{dd}=0$, see Fig. 17. This actually provides a strong numerical evidence that the periodic evolution even with $A^{dd}=-2B^{dd}$ included is stable.

Above all, the investigation on the chain-length dependence provides clear evidence that the calculated coherence evolutions in the main text are intrinsic.

[1] A. O. Caldeira and A. J. Leggett, Ann. Phys. (N.Y.) **149**, 374 (1983).
[2] B. E. Kane, Nature (London) **393**, 133 (1998).
[3] D. Loss and D. P. DiVincenzo, Phys. Rev. A **57**, 120 (1998).
[4] W. A. Coish and D. Loss, Phys. Rev. B **70**, 195340 (2004).
[5] W. M. Witzel, R. de Sousa, and S. Das Sarma, Phys. Rev. B **72**, 161306(R) (2005).
[6] W. M. Witzel and S. Das Sarma, Phys. Rev. B **74**, 035322 (2006); Phys. Rev. B **77**, 165319 (2008).
[7] S. K. Saikin, Wang Yao, and L. J. Sham, Phys. Rev. B **75**, 125314 (2007).
[8] A. M. Tyryshkin, S. A. Lyon, A. V. Astashkin, and A. M. Raitsimring, Phys. Rev. B **68**, 193207 (2003); E. Abe, A. Fujimoto, J. Isoya, S. Yamasaki, and K. M. Itoh, arXiv:cond-mat/0512404 (unpublished).
[9] Wang Yao, Ren-Bao Liu, and L. J. Sham, Phys. Rev. B **74**, 195301 (2006).
[10] D. Rossini, T. Calarco, V. Giovannetti, S. Montangero, and R. Fazio, Phys. Rev. A **75**, 032333 (2007); H. T. Quan, Z. Song, X. F. Liu, P. Zanardi, and C. P. Sun, Phys. Rev. Lett. **96**, 140604 (2006).
[11] F. M. Cucchietti, S. Fernandez-Vidal, and J. P. Paz, Phys. Rev. A **75**, 032337 (2007).
[12] Wang Yao, Ren-Bao Liu, and L. J. Sham, Phys. Rev. Lett. **98**, 077602 (2007); Ren-Bao Liu, Wang Yao, and L. Sham, New J. Phys. **9**, 226 (2007).
[13] A. J. Daley, C. Kollath, U. Schollwöck, and G. Vidal, J. Stat. Mech.: Theory Exp. 2004, 005 (2004); S. R. White and A. E. Feiguin, Phys. Rev. Lett. **93**, 076401 (2004).
[14] M. Suzuki, Prog. Theor. Phys. **56**, 1454 (1976); H. F. Trotter, Proc. Am. Math. Soc. **10**, 545 (1959).
[15] D. Gobert, C. Kollath, U. Schollwöck, and G. Schütz, Phys. Rev. E **71**, 036102 (2005).
[16] K. Hepp, Helv. Phys. Acta **45**, 237 (1972).
[17] J. S. Bell, Helv. Phys. Acta **48**, 93 (1975).
[18] M. Namiki and S. Pascazio, Phys. Rev. A **44**, 39 (1991).
[19] T. Kobayashi, Found. Phys. Lett. **5**, 265 (1992).
[20] H. Nakazato and S. Pascazio, Phys. Rev. Lett. **70**, 1 (1993).
[21] C. P. Sun, Phys. Rev. A **48**, 898 (1993).
[22] C. P. Sun, D. L. Zhou, S. X. Yu, and X. F. Liu, Eur. Phys. J. D **13**, 145 (2001).
[23] R. de Sousa and S. Das Sarma, Phys. Rev. B **68**, 115322 (2003).
[24] G. Feher, Phys. Rev. **114**, 1219 (1959).
[25] O. Morsch and M. Oberthaler, Rev. Mod. Phys. **78**, 179 (2006).